Traumatology and Orthopaedics of Kazakhstan
ISSN - e2789-9640

Original article

Participant-Specific Recognition of Grasp Type and Self-Scaled Effort Using Surface Electromyography: A Proof-of-Concept Study for Prosthetic Control in People with Congenital or Acquired Upper-Limb Absence

Ayaulym Assylbekova [1], Darkhan Zholtayev [2], Aiman Ozhikenova [3], Zhadyra Alimbayeva [4], Erik Baizhunussov [5], Sain Shaikhiyev [6], Assylbek Ozhiken [7*]

Received: August 04, 2026
Revised: August 21, 2026
Accepted: September 14, 2026
Published: October 28, 2026

Citation: Ayaulym Assylbekova, Darkhan Zholtayev, Aiman Ozhikenova, Zhadyra Alimbayeva, Erik Baizhunussov, Sain Shaikhiyev, Assylbek Ozhiken. Participant-Specific Recognition of Grasp Type and Self-Scaled Effort Using Surface Electromyography: A Proof-of-Concept Study for Prosthetic Control in People with Congenital or Acquired Upper-Limb Absence. Trauma & Ortho Kaz, 2026, 77 (5), jto067. https://doi.org/10.52889/1684-9280-2026-77-5-jto067

This work is licensed under a Creative Commons Attribution 4.0 International License

[1] Student (MSc in Applied Artificial Intelligence), School of Artificial Intelligence and Data Science, Astana IT University, Astana, Kazakhstan. E-mail: ayaulymassylbekova35@gmail.com
[2] Assistant Professor, School of Artificial Intelligence and Data Science, Astana IT University, Relive Research, Astana, Kazakhstan. E-mail: darkhan.zholtayev@astanait.edu.kz
[3] Director, Qazaq Youth Science Hub, Almaty, Kazakhstan. E-mail: a.ozhikenova@satbayev.university
[4] Leading Researcher, Satbayev University, Almaty, Kazakhstan. E-mail: zh.alimbayeva@satbayev.university
[5] Chairperson of the Board, Salidat Kairbekova National Scientific Center for Health Development, Astana, Kazakhstan. E-mail: e.baizhunussov@nrchd.kz
[6] Deputy Chairperson of the Board, Salidat Kairbekova National Scientific Center for Health Development, Astana, Kazakhstan. E-mail: s.shaikhiyev@nrchd.kz
[7] Lecturer, Qazaq Youth Science Hub, Almaty, Kazakhstan. E-mail: a.ozhiken@satbayev.university

*** Corresponding author:** a.ozhiken@satbayev.university

Abstract

Objective. To assess participant-specific recognition of grasp type and subjectively scaled effort using surface electromyography in adults without upper-limb amputation, and unintended outputs during ordinary movements. This study is a preliminary step toward prosthetic control for people with congenital or acquired upper-limb absence.

Methods. Four adults without upper-limb amputation performed eight command states: rest, open hand, and power grasp and tip pinch at low, medium and high verbally instructed effort. Effort categories were subjective; mechanical force was not measured. A separate linear discriminant analysis model was trained for each participant using time-domain features from consecutive signal windows, followed by causal majority voting over twenty windows. Evaluation comprised held-out trials separated from model fitting, newly recorded command trials processed causally, and ordinary movements without control intent; a confidence threshold of 0.60 was applied retrospectively to the latter. All recordings were obtained during one visit. No physical prosthesis was actuated. Results were summarized descriptively.

Results. On held-out trials, mean balanced accuracy was 0.810 for raw windows, 0.823 after majority voting, and 0.875 for trial-level decisions. Among outputs with correctly recognized grasp type, effort recognition was more accurate for power grasp (0.970) than tip pinch (0.706). On newly recorded command trials, mean balanced accuracy was 0.902 and trial accuracy was 0.939; at the confidence threshold, coverage was 0.925 and end-to-end accuracy was 0.862. During ordinary movements, the mean proportion of unintended active outputs was 35.6% and decreased to 22.3% after confidence rejection, which retained 81.3% of outputs. The longest uninterrupted active-output episode after rejection lasted 7.25 seconds.

Conclusion. The participant-specific decoder recognized instructed grasp and effort categories under controlled conditions. Unintended outputs during ordinary movements

remain a concern for potential prosthetic use. These results do not establish clinical benefit or prosthesis control; evaluation with intended users, physical devices and functional tasks is needed.
Keywords: electromyography, artificial limbs, machine learning, wearable electronic devices, discriminant analysis, upper extremitye.

1. Introduction

Upper-limb loss can substantially restrict object manipulation, occupational activity, and independence in everyday life. Although modern multifunctional hand prostheses can provide several grasp configurations, their practical value depends on whether the user can control them intuitively, responsively, and reliably. Myoelectric pattern recognition has long been investigated as a means of translating muscle activity into multiple prosthetic commands [1]. Nevertheless, robustness outside controlled laboratory conditions remains a central obstacle to routine clinical use [2–4]. The overall problem is therefore not simply how to reproduce hand motion, but how to decode multidimensional motor intent reliably enough to support functional prosthesis control.

Surface electromyography (sEMG) records electrical activity generated by contracting muscles through electrodes placed on the skin over the forearm or residual limb. Conventional amplitude-based control links signal magnitude to a small set of direct commands, whereas pattern-recognition systems segment multichannel signals, extract descriptive features, and classify a broader set of gestures, wrist movements, or grasp types. Compact time-domain descriptors and linear discriminant analysis remain established options for real-time myoelectric decoding [5]. Reviews describe both such classical pipelines and deep architectures that learn spatial or temporal representations directly from the signal [2–4,6]; however, reported advantages are not directly transferable across studies, because performance depends on the gesture set, channel configuration, participant population, training volume, and evaluation protocol. Robustness remains a limitation even when laboratory accuracy is high: changes in arm posture, fatigue, electrode position, and recording session alter the signal distribution presented to a trained classifier [7]. Participant-specific training reduces inter-participant variability, but it does not remove these within-participant sources of drift. Moreover, successful gesture recognition identifies what action is intended, not how strongly it should be executed.

The acquisition interface determines how much spatial information is available to the decoder and how complex the recording setup becomes. High-density surface electromyography provides richer spatial sampling, but it also increases the number of recording sites, data volume, processing demands, and placement requirements. Integrated low-density armbands consolidate electrodes within a wearable form factor, although a smaller channel count can reduce class separability. Online prosthesis testing has shown that increasing the channel count from eight to sixteen can improve some control outcomes [8], while medium-density armbands have been proposed as an intermediate design space between sparse and high-density acquisition [9]. The present study uses a circumferential armband with eight integrated dry-contact electrodes as a compact research interface, which eliminates the need to position separate disposable electrode pads. Because donning time, comfort, and long-term use were not evaluated, the device is not claimed to be more convenient for daily use.

Decoder design creates a related trade-off. Deep architectures can learn complex spatial and temporal representations, whereas classical pipelines use engineered features and comparatively simple decision functions [4, 9]. Deep models are not inherently unsuitable for real-time control, and the present study did not benchmark their inference time. For a small participant-specific dataset and a constrained wearable implementation, compact time-domain features and linear discriminant analysis were therefore selected as a deliberately lightweight design [5]. Temporal majority voting was used only to aggregate consecutive outputs from this single participant-specific classifier; it was not an ensemble of independently trained models.

Most surface-electromyography pattern-recognition studies formulate motor intent primarily as a gesture, wrist movement, or grasp class [2–4], and gesture identity alone does not specify the intended contraction intensity. Intensity has been operationalized using several non-equivalent targets. Leone et al. recorded grasp force with external sensors and trained grasp-specific force classifiers for able-bodied participants and participants with transradial amputation [10,11]. Stefanelli et al. addressed mechanically calibrated force and aperture with displacement myography, which is a different sensing modality rather than simply a higher-powered surface-electromyography system [12]. Zhou et al. instead

https://doi.org/10.52889/1684-9280-2026-77-5-jto067

classified shoulder-abduction levels defined as percentages of maximum voluntary contraction [13]. Billardello et al. provide the closest precedent for participant-defined intensity, because participants initially selected comfortable low, medium, and high contraction levels according to perceived exertion; their subsequent acquisition, however, used electromyography-based visual targets and reported activation relative to maximum voluntary contraction [14]. Mechanical force, normalized activation, and categorical intensity therefore represent related but different prediction targets. A purely verbal self-scaling protocol, in which low, medium, and high are subjective ordinal commands without force sensing or maximum-voluntary-contraction calibration, provides neither an external force reference nor physiological calibration. A decoder trained under such a protocol recognizes intended effort categories, not mechanical grasp force.

Joint grasp–effort commands can be decoded with a flat classifier, which assigns each grasp–effort combination directly to one class and thereby measures end-to-end command recognition, or with a hierarchical system that first recognizes the grasp and then applies an intensity classifier conditional on that decision [10,11,14]. Decomposition may simplify the conditional task, but an incorrect first-stage grasp prediction necessarily propagates to the final command; conditional intensity accuracy and complete joint-command accuracy therefore answer different questions. Leone et al. reported high grasp-specific force-classification performance in able-bodied participants and later demonstrated the real-time feasibility of hierarchical decoding in participants with transradial amputation [10,11], and Billardello et al. similarly combined onset detection and gesture recognition with grasp-specific intensity classifiers [14]. In contrast, Stefanelli et al. examined a compound-label formulation and found that recognition of the complete 33-configuration task was more difficult than force discrimination under fixed gesture and aperture conditions [12]. It remains unclear whether the advantage of separating gesture identity from intensity extends to verbally instructed self-scaled effort, which lacks the external calibration used in force-based studies.

Evaluation design further determines what can legitimately be inferred. Public resources such as NinaPro provide repeated movement acquisitions for reproducible analysis [15], but overlapping windows from the same contraction are strongly correlated. Allocating such windows randomly between training and testing can overestimate generalization, whereas cross-trial evaluation asks whether a decoder recognizes newly performed repetitions [16]. Qiu et al. kept all overlapping windows from the same movement within one fold to prevent temporal leakage and evaluated generalization within participants, across days, and across participants [17]. Even trial-separated offline testing remains different from causal processing of newly recorded signals and from closed-loop control of a physical prosthesis; controller delay can impair real-time control even when longer analysis windows reduce classification error [18]. Guided commands, moreover, assume that the participant is attempting one of the trained commands, and they do not show how a closed-set decoder behaves during ordinary movements when no command is intended. A trained rest class and the absence of control intent are not interchangeable: ordinary arm repositioning, object contact, and stabilization can generate activation patterns that differ from structured rest. Niu et al. showed that dynamic arm movement can reduce recognition even while participants deliberately maintain a target gesture [19], which tests preservation of an intended command under motion, whereas daily movement without intentional control tests the complementary risk of unintended command generation. Confidence rejection and temporal voting can reduce false actuation, but only by introducing coverage and latency trade-offs [20].

For people with congenital upper-limb absence or acquired loss after trauma or other causes, rehabilitation and prosthetic selection must account for the level of limb absence, available residual musculature, comfort, and the activities meaningful to the individual. In a multicentre survey of people with upper-limb absence, insufficient functionality was a reported reason for prosthesis abandonment [21]. A survey of veterans with unilateral major upper-limb amputation associated non-use of a prosthesis with greater reported activity difficulty and a greater need for help with daily activities; its observational design does not establish causation [22]. Recognition of grasp and intended effort may eventually contribute to more flexible control, but this requires direct evaluation of functional performance and the user experience in the intended population.

Previous studies have therefore established surface-electromyography gesture recognition, wearable acquisition at different channel densities, grasp-dependent force decoding, and several approaches to temporal stabilization and rejection. However, limited evidence characterizes the same compact participant-specific decoder across trial-separated locked testing, causal decoding of newly recorded grasp–effort commands, and ordinary movements performed without control intent when

effort is verbally instructed rather than mechanically calibrated. The present study addresses this gap using an eight-channel wearable interface and one participant-specific linear discriminant analysis classifier per participant. The decoder is a flat eight-class classifier; self-scaled effort is treated as an intended ordinal command rather than as measured force, and grasp and conditional-effort metrics are used only to identify the sources of its classification errors. The scope of the study does not extend to generalization across unseen participants or to clinical prosthesis use.

The aim of this study was to evaluate the feasibility and limitations of participant-specific recognition of eight command states using an eight-channel wearable surface-electromyography interface under trial-separated offline evaluation, guided online testing, and ordinary movements performed without control intent. The intended application is the future development of prosthetic control for people with congenital or acquired upper-limb absence; the present evaluation involved adults without upper-limb amputation. The eight command states comprised rest, open hand, and power-grasp and tip-pinch commands performed at low, medium, and high verbally instructed effort.

2. Materials and methods

Study design

This was a single-visit, participant-specific proof-of-concept study with three evaluation settings: trial-separated offline evaluation of structured recordings, guided online testing of newly recorded trials, and recordings of ordinary movements performed without control intent. All procedures were completed during the same visit without removing the armband, and no physical prosthesis was actuated.

Participants

Four adults without upper-limb amputation participated in the study. P01 was a 22-year-old woman, P02 was a 52-year-old woman, P03 was a 33-year-old man, and P04 was a 24-year-old man. All participants were right-handed. Surface electromyography was recorded from the right forearm. Participants were recruited by convenience, and no additional formal inclusion or exclusion criteria were applied.

Ethical considerations

The study was conducted in accordance with the principles of the Declaration of Helsinki. Informed consent was obtained from all participants before participation.

Surface-electromyography acquisition setup

Surface electromyography was recorded using an OYMotion gForce Pro forearm armband with eight integrated dry-contact electrodes. All eight channels were active. The armband was placed circumferentially around the proximal right forearm, below the elbow, and secured with an elastic wrap and metal clip to reduce slipping and rotation. Figure 1 shows the device and its placement.

The armband remained in place throughout the structured acquisition, guided online testing and ordinary-movement recordings. All three procedures were completed during the same visit without removing and re-donning the device. The exact distance from the elbow and the anatomical alignment of individual channels were not recorded. Electrode displacement was also not measured.



Figure 1 - Surface electromyography device and fixation: a – the OYMotion gForce Pro armband used for signal acquisition; b – the armband positioned on the proximal right forearm and secured with an elastic wrap and metal clip

Command states and experimental protocol

The classifier distinguished eight command states. These comprised rest, open hand, and two grasp types performed at three effort levels. The grasp types were power grasp and tip pinch. The effort levels were low, medium, and high. Power grasp involved whole-hand closure, whereas tip pinch involved the thumb and index finger. For rest, participants relaxed the hand and forearm. For open hand, participants opened the hand without intentionally producing a grasp.

https://doi.org/10.52889/1684-9280-2026-77-5-jto067

During active grasp trials, participants manipulated a nearly empty plastic bottle. The bottle served as a lightweight, compliant object that made the hand–object interaction visible. It was not instrumented with a force sensor. Figure 2 shows representative executions of the grasp–effort commands.



a *b* *c*

Figure 2 - Representative task execution: a – power grasp at the high verbally instructed effort target; b – tip pinch at the low target; c – tip pinch at the medium target. The nearly empty plastic bottle was a lightweight demonstration object and was not instrumented to measure or calibrate force

During active grasp trials, participants received verbal instructions to produce low, medium, or high effort. The corresponding targets were approximately 2–3/10, 4–6/10, and 7–8/10. After each active trial, participants independently rated their perceived effort using an integer from 1 to 10. They could also leave the response blank. Class labels were defined by the instructed effort level and were not changed by the post-trial ratings. Mechanical grasp force and maximum voluntary contraction were not measured.

Before structured acquisition, each participant completed three recorded practice trials: one power-grasp trial at low effort, one at medium effort, and one at high effort. The practice trials were not included in model development or evaluation. The structured acquisition contained 64 planned trials. Each of the eight command states was repeated eight times. The trials were organized into eight rounds, with each round containing one trial from every command state. Class order was randomized within each round using a fixed seed. Each trial included a transition into the instructed state, a 5-s steady-hold phase, and a release phase. For active commands, participants gradually increased their contraction during the transition. The ramp-up lasted approximately 1.5 s for P01 and 4.0 s for P02–P04. Only the 5-s steady-hold phase was included in the primary classification analysis.

Participants rated their current fatigue on a scale from 0 to 10 after each block of 16 structured trials, including the final block. These ratings were used only to monitor participant well-being. They were not used as class labels or model inputs. After each non-final block, a 90-s rest break began once the fatigue rating had been collected.

During data collection, the operator flagged trials when participants forgot the prompted action, performed it incorrectly, or appeared to change the instructed effort. Suspected effort changes were identified from participant reports or visible changes in bottle deformation observed by the operator. Bottle deformation was used only as a qualitative cue for trial quality control. It was not measured or used to assign effort levels. Trials marked with either a warning or a failure were excluded from model development and evaluation. Missing post-trial effort ratings alone did not lead to trial exclusion. These ratings were not imputed.

Data partitioning and participant-specific workflow

Split assignment was determined by acquisition round before quality control. Rounds 1–4 formed the training subset, rounds 5–6 formed the validation subset, and rounds 7–8 formed the locked-test subset. The planned split therefore contained four training, two validation, and two locked-test trials per class. This corresponded to 32 training, 16 validation, and 16 locked-test trials for each participant. All windows derived from the same trial remained within its assigned subset. Quality-control exclusions removed complete trials and did not reassign trials between subsets.

A separate preprocessing configuration, feature scaler, and classifier were created for each participant.

https://doi.org/10.52889/1684-9280-2026-77-5-jto067

Model development used only the retained training trials. Four-fold cross-validation was performed within this subset. Trials were assigned to folds by trial ID, with class proportions balanced as closely as possible. All windows from the same trial remained in one fold. Validation trials were not included in cross-validation.

Linear discriminant analysis (LDA) was selected as the primary classifier before the comparative evaluation because of its widespread use in sEMG-based gesture recognition and computational efficiency. Wang et al. [23] provide this rationale, citing earlier research reporting performance comparable to more complex classifiers with lower computational time. A support vector machine with a radial basis function kernel (RBF-SVM) was included as a comparator. Both classifiers used an adapted present–past log-transformed (PPaL) representation, which combines log-transformed features from the current and immediately preceding signal windows, as described in the Feature extraction subsection. Cross-validation assessed development performance and was not used to select the primary classifier. No hyperparameters were tuned using the validation or locked-test subsets.

Validation predictions were generated using participant-specific LDA pipelines fitted only on the retained training trials. These predictions were used for the post hoc confidence-threshold sensitivity analysis. The final scaler and LDA classifier were then refitted on the combined retained training and validation trials. The locked-test subset was evaluated once using this final pipeline. The same fixed pipeline was subsequently applied to guided online trials and ordinary-movement recordings.

Table 1 - Protocol and retained structured trials

Participant	Planned	Retained	Training	Validation	Locked test	Final fit
P01	64	61	29	16	16	45
P02	64	62	30	16	16	46
P03	64	62	31	16	15	47
P04	64	64	32	16	16	48

Note. Values represent numbers of trials. The final fit combined the retained training and validation trials. Locked-test trials were not used for model fitting or preprocessing decisions

Participant-level trial counts before and after quality control are presented in Table 1.

Figure 3 summarizes the participant-specific development and evaluation workflow and the signal-processing pipeline described in the following subsections.

After the participant-specific filtering configuration was fixed, each channel was processed using a fourth-order causal Butterworth band-pass filter with a passband of 20–200 Hz. When enabled, the notch filter was applied after the band-pass filter.

For structured trials, the steady-hold segment was identified from the recorded phase markers and selected before preprocessing. Its nominal duration was 5 s. Each selected segment was processed separately using the filters described above. Filter states were initialized to zero at the beginning of each segment. The first 500 ms of the filtered segment were discarded to reduce start-up transients.

Each ordinary-movement recording was processed as a separate continuous signal. Filter states were initialized to zero at the beginning of the recording. The first 500 ms of the filtered signal were discarded before feature extraction.

Guided online data were processed as a continuous stream. Filter states were initialized to zero once when the online processor started. They were retained across consecutive signal blocks and trials. The 500-ms warm-up period was applied only once at the start of online processing.

Feature extraction

Across all evaluation settings, signals were divided into overlapping 150-ms analysis windows with a 50-ms step. At a sampling rate of 500 Hz, each window contained 75 samples and advanced by 25 samples. For structured trials, windows were extracted from the preprocessed steady-hold segments described in the Signal preprocessing subsection. Ordinary-movement recordings and guided online signals were processed continuously; the selection of guided online outputs for evaluation is described in the Guided online evaluation subsection.

Five time-domain features were calculated separately for each of the eight surface electromyography channels: mean absolute value, root mean square, waveform length, zero crossings, and slope sign changes. A threshold of 5 analogue-to-digital converter units was used when counting zero crossings and slope sign changes. Together, these features formed a 40-dimensional TD5 vector for each window.

https://doi.org/10.52889/1684-9280-2026-77-5-jto067

An adapted version of the present–past log-transformed (PPaL) representation proposed by Rasines et al. [24] was used to include short-term temporal information. In the original formulation, the feature vectors from the current and immediately preceding windows were concatenated and transformed using the logarithm of the squared feature values. In the present implementation, each TD5 value was clipped to be non-negative and transformed using the natural logarithm of one plus the feature value. The transformed vectors from the current and preceding windows were then concatenated to produce an 80-dimensional input vector.

During offline processing, the previous-window component was set to zero for the first window of each trial. The same reset was applied at the beginning of each separately processed ordinary-movement recording. During guided online processing, the previous-window component was initialized as a zero vector only when the processor started. It was then retained across signal blocks and trial boundaries as part of the continuous data stream.

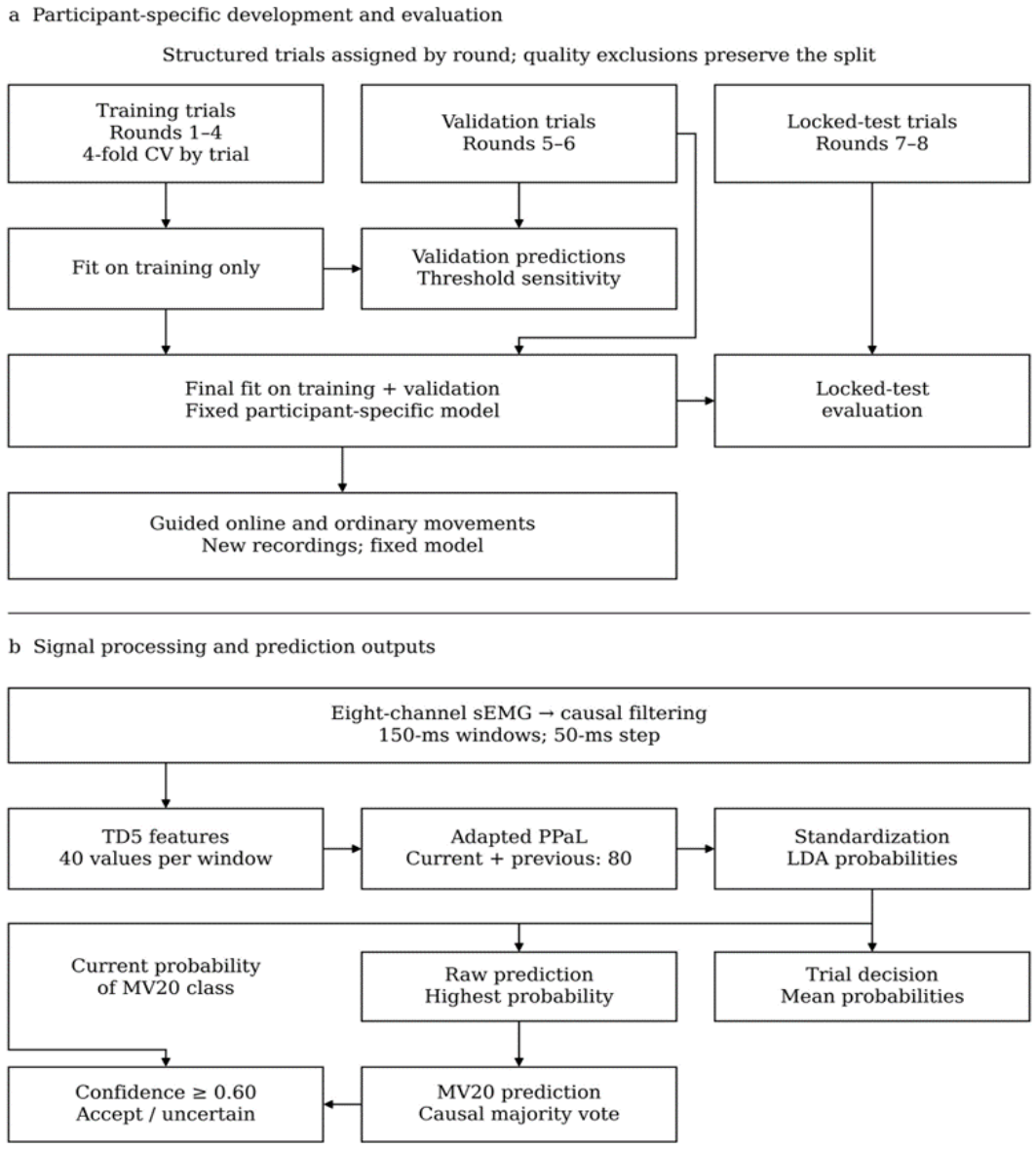


Figure 3 - Study workflow and decoding pipeline: a – participant-specific model development and evaluation; b – signal processing and prediction outputs. CV = cross-validation; sEMG = surface electromyography; TD5 = five time-domain features per channel; PPaL = present–past log-transformed representation; LDA = linear discriminant analysis; MV20 = causal majority voting over up to 20 predictions. Trial decisions use mean LDA probabilities across evaluated windows. Confidence is the current LDA probability of the MV20-selected class. The fixed 0.60 threshold was applied during guided online evaluation and retrospectively to ordinary-movement recordings

https://doi.org/10.52889/1684-9280-2026-77-5-jto067

Signal preprocessing

Signals from all eight sEMG channels were sampled at 500 Hz with 12-bit analogue-to-digital resolution. The digital midpoint of 2047.5 was subtracted from each sample.

The need for a 50-Hz notch filter was determined separately for each participant using only the retained training steady-hold segments. Power spectral density was estimated from the midpoint-subtracted, otherwise unfiltered signals using Welch's method with 1024-sample segments. The spectra were averaged across training trials for each channel. The 50-Hz peak was defined as the maximum power between 49 and 51 Hz. Background power was defined as the median power within the adjacent 45–48-Hz and 52–55-Hz bands. The peak-to-background power ratio was converted to decibels for each channel. The median across the eight channels was used as the participant-level score. A 50-Hz notch filter with Q = 30 was enabled when this score was at least 6 dB. This criterion enabled notch filtering only for P02.

Classification

A separate linear discriminant analysis classifier was trained for each participant using the 80-dimensional adapted PPaL representation. The classifier used the least-squares solver, automatic covariance shrinkage, and equal class priors of 0.125.

Features were standardized to zero mean and unit variance before classification. During development cross-validation, the scaler and classifier were fitted using only the training trials in the corresponding fold.

Each trial then contributed the same number of PPaL vectors during model fitting. This number was set to the minimum available across trials in the fitting set. For trials with more vectors, approximately evenly spaced positions were selected. This gave each trial equal weight during fitting while preserving the original previous-window information. All available vectors were retained for validation and locked-test evaluation.

Prediction aggregation

Window-level LDA predictions were smoothed using causal majority voting over the current and up to 19 preceding predictions (MV20). During the first 19 windows, the vote used all predictions available at that point. If two or more classes received the same number of votes, the class that occurred most recently was selected.

During offline evaluation, the voting history was reset at the beginning of each trial. It was also reset at the beginning of each separately processed ordinary-movement recording. During guided online evaluation, the voting history was initialized once and retained across trial boundaries as part of the continuous data stream.

With a 150-ms window and a 50-ms step, a full 20-window vote covered 1.10 s of signal context. This value describes the smoothing horizon and should not be interpreted as measured response latency. Trial-level decisions were obtained by averaging the raw LDA class probabilities across all evaluated windows within each trial. The class with the highest mean probability was selected.

Guided online evaluation

The fixed participant-specific models were evaluated on newly recorded trials. Participants selected which command to perform, and the reference class was recorded after each trial. Model predictions were not shown to either the participant or the operator during trial execution or reference labeling. Only summary performance statistics were displayed after the evaluation. Signals were processed causally, but no physical prosthesis was actuated. P01, P03, and P04 completed 16 trials each. P02 completed 17 trials, including one additional power-grasp trial at medium effort.

Only predictions generated during the 5-s steady-hold phase were included in the guided-online evaluation. Predictions generated while participants moved into the selected state or released it were excluded. Window-level balanced accuracy and trial-level accuracy were calculated before confidence rejection. Confidence-threshold coverage, accepted accuracy, and end-to-end accuracy were calculated with the fixed 0.60 rejection rule using the same evaluated predictions.

Signal processing continued throughout each trial and between trials. Filter states, the previous-window feature component, and the majority-voting history were retained. Therefore, predictions at the beginning of the steady-hold phase could still reflect signal activity and prediction history from the preceding transition.

For each window, confidence was defined as the current LDA probability assigned to the class selected by MV20. This was not necessarily the probability of the class selected by the current raw prediction. An output was accepted when its confidence was at least 0.60 and was otherwise marked as uncertain. The threshold was an unchanged software default and was not optimized using evaluation data.

Post hoc threshold sensitivity was assessed using the validation predictions described in the Data partitioning and participant-specific workflow subsection. A separate descriptive analysis applied alternative thresholds to saved guided-online predictions from the final model fitted on the retained

training and validation trials. Both analyses used the confidence definition given above and examined thresholds of 0.50, 0.60, and 0.70. Neither analysis was used to select or change the operational threshold of 0.60.

Ordinary movements without control intent

All four participants completed an ordinary-movement task lasting approximately 180 s. The instructions and target duration were the same for all participants. Participants changed arm position, rotated the forearm, and touched everyday objects. They chose their own sequence of movements and were instructed to avoid deliberately issuing any of the trained commands.

These activities could produce muscle activity without an intention to control the interface. Rest was therefore the required decoder output. Any non-rest prediction was treated as an unintended active output.

Outcome measures

Eight-class performance was evaluated using balanced accuracy, macro-F1, and class-specific precision, recall, and F1 scores. Grasp-level performance was calculated after combining the effort-specific classes into four categories: rest, open hand, power grasp, and tip pinch.

Conditional effort recognition was evaluated separately for power grasp and tip pinch. Only observations for which the grasp type was correctly recognized were included. Combined conditional effort performance pooled observations from both grasp types and excluded rest and open hand. It therefore measured effort recognition conditional on correct grasp recognition rather than overall eight-class accuracy.

For ordinal analysis, low, medium, and high effort were encoded as 0, 1, and 2. Quadratic weighted Cohen's kappa and mean absolute grade error were calculated separately for each grasp type. Errors were also classified as adjacent-level errors or extreme low–high errors. Because these analyses excluded observations with an incorrect grasp prediction, the proportion of retained grasp observations was reported as ordinal coverage.

Guided online performance was summarized using MV20 balanced accuracy, trial-level accuracy, confidence-threshold coverage, accepted accuracy, and end-to-end accuracy. Coverage was the proportion of windows with an accepted output. Accepted accuracy was calculated among accepted windows only. End-to-end accuracy treated both rejected and incorrectly classified windows as failures.

For ordinary-movement recordings, false activation rate (FAR) was first calculated separately for raw and MV20 predictions without confidence rejection. It was defined as the proportion of evaluated outputs assigned to any non-rest class.

A retrospective analysis then applied the fixed confidence threshold of 0.60 to MV20 outputs from the saved participant-specific models. The models were not retrained. Confidence was calculated as described in the Guided online evaluation subsection. After rejection, false activation rate was defined as the number of accepted non-rest outputs divided by the total number of evaluated outputs. Coverage, accepted-rest fraction, and rejected-output fraction were also calculated using this denominator.

For MV20, activation episodes were evaluated both before and after confidence rejection. Consecutive active outputs formed one episode. After rejection, only accepted non-rest outputs were considered active. A rest output or a rejected output ended the episode. Episode counts, approximate total active-output time, and the longest episode were reported. Approximate durations were calculated by multiplying the number of outputs by the 50-ms prediction step.

Statistical analysis

Participant-specific results were reported as the primary outcomes. Results across the four participants were summarized using the mean and sample standard deviation and, where informative, the range. For the trial-level locked-test analysis, class probabilities were averaged across windows within each trial, and the class with the highest mean probability was selected. A 95% confidence interval for participant-mean balanced accuracy was estimated with 5,000 hierarchical bootstrap iterations (random seed 20260905). In each iteration, participants were sampled with replacement, followed by trials with replacement within each sampled participant and true class, retaining the observed number of trials in each class. Balanced accuracy was calculated for each sampled participant as the mean recall across the eight classes, and then averaged across the sampled participants. The 2.5th and 97.5th percentiles of the bootstrap distribution formed the interval. The interval was interpreted descriptively given the four participants. Given the small sample, differences between power grasp and tip pinch and between raw and MV20 performance were interpreted descriptively.

No population-level hypothesis tests were performed. Window-level outputs were not treated as independent observations because adjacent windows overlapped and multiple windows originated from the same trial or recording.

https://doi.org/10.52889/1684-9280-2026-77-5-jto067

3. Results

Data retention and self-reported effort

After quality control, retained structured-trial totals were 61/64 for P01, 62/64 for P02, 62/64 for P03, and 64/64 for P04. All 16 planned validation trials were retained for each participant. The locked test contained 16 trials for P01, P02, and P04 and 15 for P03, yielding 63 trials overall.

Self-reported perceived-effort ratings were summarized across all 192 planned active structured trials before quality-control exclusions; ratings were available for 188 trials. The four missing ratings were from P03 trials that passed quality control; they remained missing without imputation and did not affect trial inclusion. Ratings generally increased across verbally instructed levels (Figure 4). Some high-effort trials received ratings of 9 or 10. These distributions are descriptive because the verbal target, not the post-trial rating, defined the class.

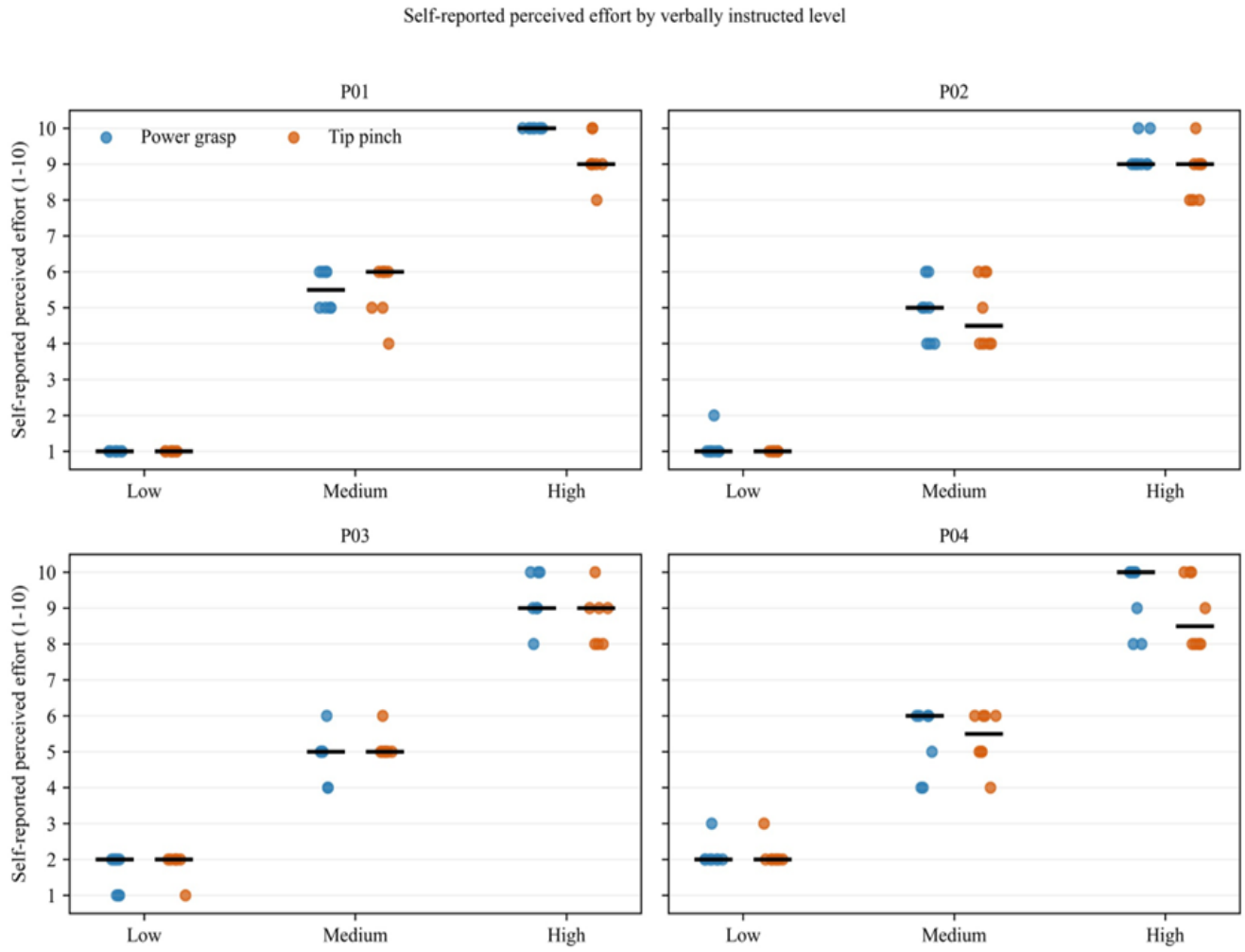


Figure 4 - Post-trial self-reported perceived effort by verbally instructed target level and grasp. Points represent trials, and summary marks are descriptive; ratings did not generate class labels

Locked-test eight-class performance

Participant-mean locked-test balanced accuracy was 0.810 ± 0.048 for raw windows, 0.823 ± 0.062 after MV20, and 0.875 ± 0.072 for trial decisions (Table 2). The class-stratified hierarchical bootstrap 95% confidence interval for participant-mean trial-level balanced accuracy was 0.797–0.953. MV20 increased mean balanced accuracy by 1.3 percentage points compared with raw predictions. Its effect varied across participants. The pooled class-wise pattern is shown in Figure 5.

https://doi.org/10.52889/1684-9280-2026-77-5-jto067

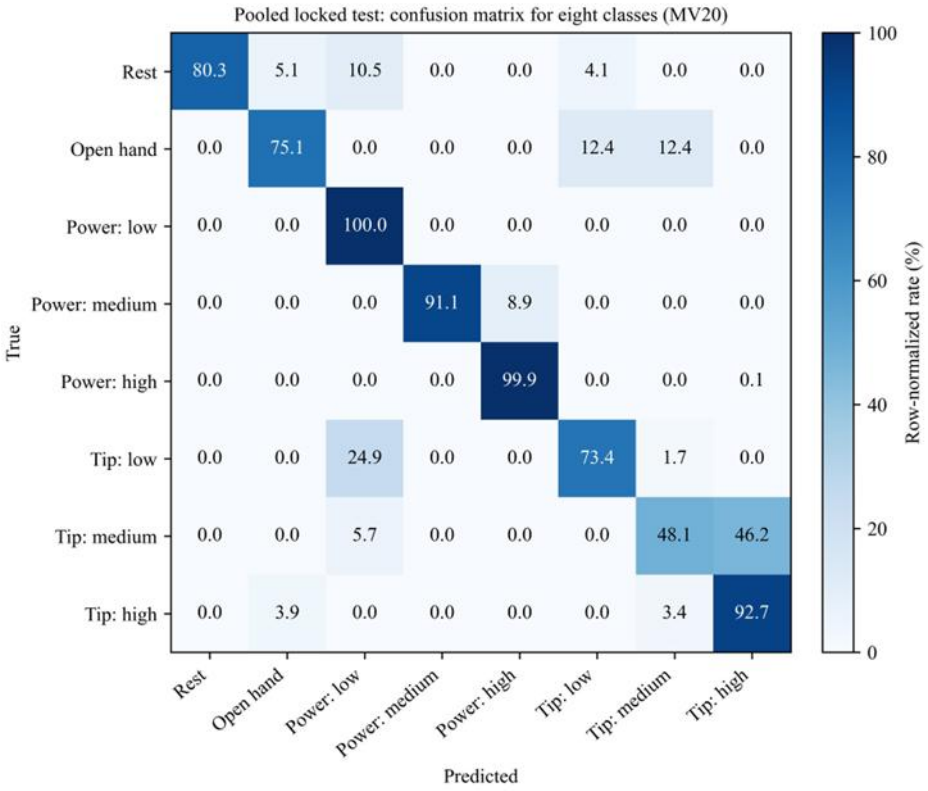


Figure 5 - Pooled locked-test confusion matrix for the eight classes after causal twenty-window majority voting. Rows are normalized by true class. Unit: window; the pooled display is descriptive because windows are clustered within trials and participants

Table 2 - Participant-wise locked-test performance of the primary classifier

Participant	Raw BA	Raw macro-F1	MV20 BA	MV20 macro-F1	Trial BA	Trial macro-F1
P01	0.869	0.870	0.907	0.905	0.938	0.933
P02	0.763	0.754	0.765	0.753	0.812	0.792
P03	0.829	0.819	0.829	0.808	0.938	0.917
P04	0.780	0.745	0.790	0.746	0.812	0.767
Mean ± SD	0.810 ± 0.048	0.797 ± 0.059	0.823 ± 0.062	0.803 ± 0.074	0.875 ± 0.072	0.852 ± 0.085

Note. BA = balanced accuracy; macro-F1 = unweighted mean of class-specific F1 scores, each calculated as the harmonic mean of precision and recall; MV20 = causal twenty-window majority voting; SD = sample standard deviation

Grasp and conditional effort decomposition

At the MV20 level, mean joint eight-class balanced accuracy was 0.823 ± 0.062, grasp balanced accuracy was 0.860 ± 0.088, and combined conditional effort balanced accuracy was 0.838 ± 0.080. Conditional effort recognition differed descriptively by grasp: power-grasp balanced accuracy was 0.970 ± 0.035, compared with 0.706 ± 0.144 for tip pinch. Participant-specific tip-pinch effort balanced accuracy ranged from 0.593 to 0.916, whereas power-grasp effort balanced accuracy ranged from 0.928 to 1.000. With four participants, this difference is an observed within-sample pattern rather than evidence of population-level superiority. Table 3 summarizes the group-level decomposition.

Ordinal effort errors

Among MV20 predictions that retained the correct grasp identity, no pooled error directly crossed between low and high effort (Figures 6 and 7). All observed ordinal mistakes were adjacent low–medium or medium–high errors. This result must be read together with ordinal coverage: retained-grasp coverage was high for power grasp and generally lower or more variable for tip pinch, particularly for P02.

https://doi.org/10.52889/1684-9280-2026-77-5-jto067

The zero extreme-error rate therefore does not imply that every power or tip observation received an effort prediction; grasp-confused observations were outside the conditional ordinal calculation.

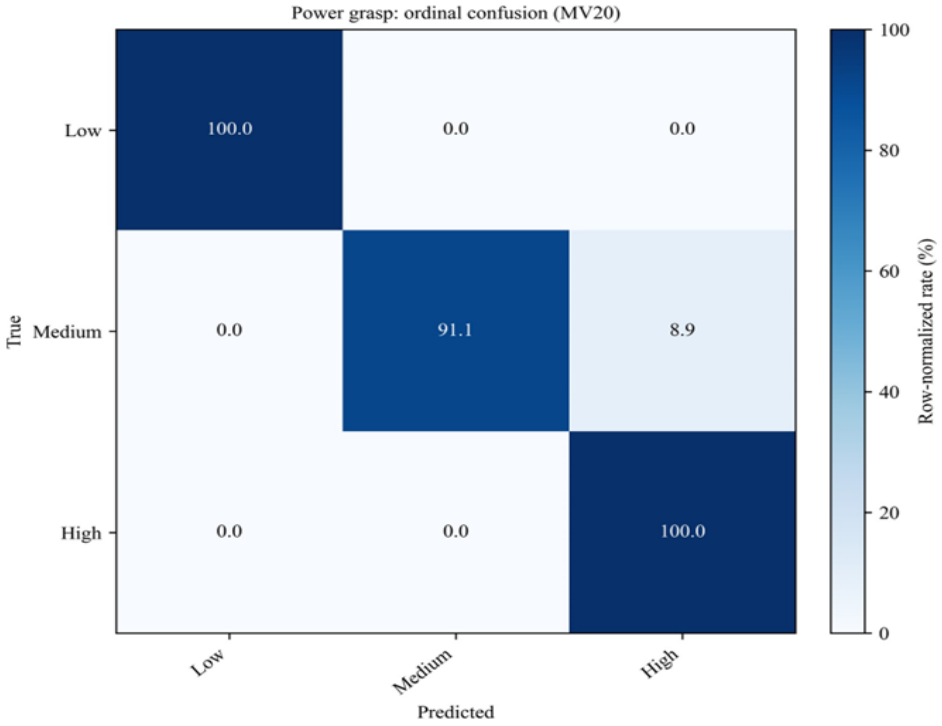


Figure 6 - Ordinal confusion matrix for power-grasp effort after causal twenty-window majority voting among predictions retaining the correct grasp identity. Rows are normalized by true effort level; coverage must accompany interpretation

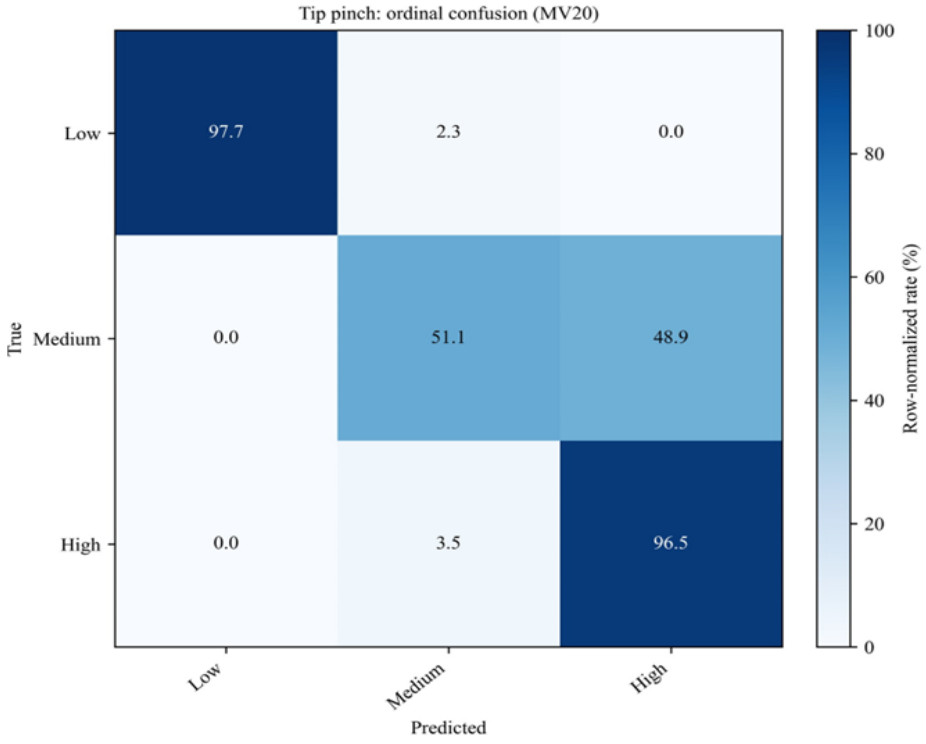


Figure 7 - Ordinal confusion matrix for tip-pinch effort after causal twenty-window majority voting among predictions retaining the correct grasp identity. Rows are normalized by true effort level; coverage must accompany interpretation

https://doi.org/10.52889/1684-9280-2026-77-5-jto067

Table 3 - Group-level locked-test performance and task decomposition

Outcome	Aggregation	Mean ± SD
Joint eight-class BA	Raw window	0.810 ± 0.048
Joint eight-class BA	Causal MV20	0.823 ± 0.062
Joint eight-class BA	Trial decision	0.875 ± 0.072
Joint eight-class macro-F1	Raw window	0.797 ± 0.059
Joint eight-class macro-F1	Causal MV20	0.803 ± 0.074
Joint eight-class macro-F1	Trial decision	0.852 ± 0.085
Grasp BA	Causal MV20	0.860 ± 0.088
Combined conditional effort BA	Causal MV20	0.838 ± 0.080
Power-grasp effort BA	Causal MV20	0.970 ± 0.035
Tip-pinch effort BA	Causal MV20	0.706 ± 0.144

Note. BA = balanced accuracy; macro-F1 = unweighted mean of class-specific F1 scores, each calculated as the harmonic mean of precision and recall; MV20 = causal twenty-window majority voting; SD = sample standard deviation. Conditional effort metrics include only observations with correctly recognized grasp type and exclude rest and open hand

Guided online performance

On newly recorded guided trials, participant-mean MV20 window balanced accuracy was 0.902 ± 0.076 and trial accuracy was 0.939 ± 0.070 (Table 4). P01 and P04 reached trial accuracy of 1.000; P02 and P03 reached 0.882 and 0.875. At the operational confidence threshold of 0.60, coverage averaged 0.925 ± 0.042 and end-to-end accuracy averaged 0.862 ± 0.091. These are guided online results without physical prosthesis actuation.

Post hoc sensitivity analysis of validation predictions from models fitted using retained training trials only gave coverage of 0.933 ± 0.014, accepted-output accuracy of 0.888 ± 0.053, and end-to-end accuracy of 0.828 ± 0.047 at the 0.60 threshold. Across the examined thresholds of 0.50, 0.60, and 0.70, higher thresholds increased accepted-output accuracy but reduced coverage and end-to-end accuracy. These validation analyses were descriptive and were not used to change the operational threshold of 0.60.

Table 4 - Group-level guided online performance

Outcome	Mean ± SD
MV20 window BA	0.902 ± 0.076
Trial accuracy	0.939 ± 0.070
Coverage at 0.60	0.925 ± 0.042
End-to-end accuracy at 0.60	0.862 ± 0.091

Note. BA = balanced accuracy; MV20 = causal twenty-window majority voting. The 0.60 threshold was an unchanged operational software default

A separate descriptive analysis applied alternative thresholds to saved guided-online predictions from the final model fitted using retained training and validation trials. Across the four participants, thresholds of 0.50, 0.60, and 0.70 produced mean coverage of 0.938, 0.925, and 0.906, respectively; mean accepted-output accuracy of 0.926, 0.931, and 0.937; and mean end-to-end accuracy of 0.871, 0.862, and 0.851. Higher thresholds increased accuracy among accepted outputs while reducing coverage and end-to-end accuracy. This guided-online threshold comparison was not used to select or change the operational threshold of 0.60.

Daily movements without intentional commands

Daily-movement evaluation revealed frequent active outputs despite the absence of intentional control commands. Before confidence rejection, raw FAR was 0.359 ± 0.095 and MV20 FAR was 0.356 ± 0.114; both rates used all evaluated outputs as the denominator. Participant MV20 FAR ranged from 25.3% for P04 to 51.9% for P02.

Applying the fixed confidence threshold of 0.60 retrospectively reduced mean MV20 FAR to 0.223 ± 0.085 while retaining 0.813 ± 0.059 of all evaluated outputs. The longest uninterrupted decoder-output

episode decreased in every participant: from 10.70 to 2.15 s for P01, from 11.40 to 2.60 s for P02, from 15.85 to 7.25 s for P03, and from 21.95 to 4.90 s for P04. The mean participant-specific maximum decreased from 14.98 ± 5.18 to 4.23 ± 2.35 s. After rejection, episode counts were 99, 199, 78, and 72 for P01–P04, respectively. Rejected outputs interrupted active sequences and could split one episode into several shorter episodes.

Participant-level variability

Performance varied substantially across individuals and outcomes. P01 had the highest locked MV20 joint balanced accuracy (0.907), while P02 had the lowest (0.765). Before confidence rejection, P04 combined lower locked joint performance (0.790) with the best guided online MV20 balanced accuracy (0.992) and the lowest daily-movement FAR (25.3%). Conversely, P02 had the highest daily-movement FAR (51.9%) and the greatest number of false episodes before rejection (38).

4. Discussion

This four-participant proof of concept showed that a lightweight participant-specific pipeline could discriminate eight joint grasp–effort states under controlled acquisition. Trial-level locked-test balanced accuracy reached 0.875 ± 0.072, with a hierarchical bootstrap interval of 0.797–0.953 for the participant mean. The interval is relatively wide and reflects both the small cohort and the limited number of locked trials. The result should therefore be interpreted as within-session feasibility rather than a population-level estimate or evidence of clinical readiness. The participant-level patterns also support participant-wise reporting and caution against treating the four-participant mean as a stable population estimate.

For rehabilitation and prosthetic practice, these results describe an early signal-decoding component rather than a demonstrated treatment. People with congenital upper-limb absence and people with acquired amputation may differ in anatomy, residual muscles, motor experience, age and rehabilitation needs; their performance cannot be inferred from four adults without amputation. Incorrect or unintended commands could interfere with object handling, and a clinically meaningful system would need reliable command rejection, acceptable response time, appropriate fitting and training, and assessment of everyday tasks with the intended users. The present experiment did not measure independence, comfort, quality of life or actual prosthetic grasp, so improvement in these outcomes cannot be claimed [21,22].

Decomposing the joint task clarified the error structure. Grasp balanced accuracy was 0.860 ± 0.088, while combined conditional effort balanced accuracy was 0.838 ± 0.080. More importantly, conditional effort performance was much higher for power grasp than for tip pinch in this sample. A whole-hand power grasp may produce broader and more separable forearm activation than a low-intensity tip pinch, while fine pinch contractions may overlap more strongly across effort levels or with other classes. This explanation is plausible but not proven by the present results because no channel-wise amplitude or muscle-specific analysis was completed. Future work should quantify normalized trial-level amplitude and grasp-specific separability.

The ordinal analysis characterizes the magnitude of errors between effort levels. No direct low-versus-high errors appeared among predictions that retained the correct grasp, indicating that the effort mistakes within this conditional subset were adjacent. This is encouraging because adjacent errors may be less disruptive than extreme reversals. However, the calculation excludes observations assigned to the wrong grasp family. Ordinal coverage is therefore essential: a perfect conditional kappa on a small retained subset does not imply reliable end-to-end control. Future reporting should keep conditional ordinal severity beside joint accuracy and grasp-retention coverage.

Causal MV20 increased mean locked balanced accuracy only from 0.810 to 0.823. In daily-movement recordings, MV20 alone did not materially reduce the overall proportion of active outputs. Retrospective confidence rejection at the fixed 0.60 threshold reduced FAR, but the longest accepted active-output episode still lasted 7.25 s for P03. A full vote spans 1.10 s of signal context, although this is not a measured response delay. Because controller delay can impair real-time control [18] and confidence-gated voting trades false actuation against rejection and latency [20], future evaluation should report measured onset-to-stable-command latency together with accuracy.

Guided online performance was strong: MV20 balanced accuracy was 0.902 ± 0.076 and trial accuracy was 0.939 ± 0.070. These newly acquired trials support causal same-setting feasibility, but they did not involve prosthetic actuation or a functional manipulation task.

At the operational 0.60 threshold, coverage was 92.5% and end-to-end accuracy was 86.2%; the latter penalizes both rejected and incorrect outputs, so

retaining most outputs did not guarantee that every retained output was correct.

The 0.60 confidence threshold was an unchanged software default and was not optimized. The retrospective validation and guided online analyses showed that higher thresholds improved accuracy among accepted outputs while reducing coverage and end-to-end accuracy. These findings characterize the effect of rejection but do not establish calibrated probabilities or an optimal threshold. A future protocol should evaluate probability calibration and select thresholds using validation data before fixing them for subsequent evaluation.

The most consequential finding was the high active-output rate during daily movements without intentional commands. MV20 FAR averaged 35.6% before confidence rejection and 22.3% after the fixed 0.60 threshold. The longest uninterrupted episode decreased for every participant, but a 7.25-s episode remained for P03. These values describe consecutive decoder outputs, not physical prosthesis movement. Such persistence is qualitatively different from isolated single-window noise. Because this study did not actuate a physical prosthesis, it does not establish suitability or unsuitability for motor control; it identifies a robustness issue that requires testing in a closed-loop prosthesis task. Confidence rejection reduced, but did not eliminate, unintended active outputs.

These recordings must not be described as complete rest. Participants moved the arm and could make real, low-intensity contractions when touching or stabilizing objects—for example, minimally closing the fingers around a handle. The label false activation is operational: the user did not intend to issue a control command, even if the muscle pattern resembled a trained grasp. This distinction separates the current question from Niu et al., who evaluated preservation of an intended gesture during arm movement [19]. Both are relevant to practical robustness, but one measures command preservation and the other unintended-command rejection.

The target construct limits numerical comparison with prior work. Leone et al. and Stefanelli et al. used mechanically referenced force [10–12], while Zhou et al. used maximum-voluntary-contraction-normalized levels [13]. Billardello et al. are closer because their contraction levels were initially selected through perceived exertion [14], but their later electromyographic visual targets and calibration still differ. The present results concern nominal self-scaled commands, not force estimation or mechanically verified effort ordering.

The lightweight design of eight channels, five time-domain features, previous-window augmentation, standardization, and linear discriminant analysis is computationally modest by architecture. However, execution time, memory use, and power consumption were not measured, so no empirical efficiency advantage over deep learning is claimed. Compactness also does not resolve distribution shift. Participant-specific preprocessing choices and divergent outcomes reinforce the personalized nature of the system. Cross-session electrode shift and redonning remain untested despite their established effect on performance [7] and their continuing importance for real-world myoelectric interfaces [25].

Several limitations are fundamental. The sample included only four able-bodied participants, formal eligibility criteria were limited, and exact channel-specific electrode placement was not recorded. There was one analysed structured acquisition session per participant, no cross-day or post-redonning test, no force sensor, no MVC measurement, no mechanically validated effort ordering, and no users with upper-limb amputation. Guided online trials did not actuate a prosthesis. The daily-movement recording was short and covered only one ordinary-movement recording per participant. Overlapping windows provide dense output traces but not independent statistical observations.

The immediate priority is explicit rejection evaluated without leakage. Probability calibration and threshold selection should use validation data, with the resulting pipeline fixed before locked, guided, and daily-movement testing. Future reporting should combine coverage, selective accuracy, FAR, switching, burst duration, and measured delay. A hierarchical decoder should be compared with the flat model on identical trial-wise folds. Subsequent work should add cross-day redonning, longer daily-activity recordings, physical-prosthesis tasks, and individualized validation with intended users.

5. Conclusion

An eight-channel wearable surface-electromyography interface with present–past log-transformed time-domain features and participant-specific linear discriminant analysis achieved feasible recognition of joint grasp and verbally instructed self-scaled effort under controlled, trial-separated conditions. Grasp recognition was more consistent than tip-pinch effort recognition, and guided online trials produced high descriptive accuracy. During ordinary movements without intentional commands, the false activation rate after twenty-window majority voting decreased from 35.6% before confidence rejection to

22.3% after the fixed 0.60 threshold, but an uninterrupted active decoder-output episode of 7.25 s remained for one participant. The current system is a participant-specific technical proof of concept; it does not estimate force or establish closed-loop prosthesis control. Progress depends on leak-free confidence calibration, explicit rejection, measured latency, cross-session testing, and validation with intended end users.

Conflict of interest. The authors declare no conflict of interest.

Funding. This work was supported by the Committee of Science of the Ministry of Science and Higher Education of the Republic of Kazakhstan under Grant BR24992820.

Author contributions. Conceptualization – D.Z., A.O.; methodology – D.Z., A.A.; software – A.A.; validation – D.Z., Zh.A.; formal analysis – A.A., D.Z.; investigation – A.A., D.Z., O.A.; resources – A.O., Zh.A.; data curation – A.A.; writing (original draft preparation) – A.A., D.Z.; writing (review and editing) – D.Z., A.O., Zh.A., O.A.; visualization – A.A.; supervision – D.Z.; project administration – A.O.,E.B., S.S. All authors have read and agreed to the final version of the manuscript and signed the copyright transfer form.

AI Declaration. The authors confirm that no generative AI tools or AI-assisted technologies were employed in the research, data analysis, interpretation of results, or preparation of this manuscript. The manuscript was developed entirely through the authors' own scholarly work and intellectual contributions.

References

1. Hudgins, B., Parker, P. K., & Scott, R. N. (1993). A new strategy for multifunction myoelectric control. IEEE Transactions on Biomedical Engineering, 40(1), 82–94. https://doi.org/10.1109/10.204774

2. Scheme, E., & Englehart, K. (2011). Electromyogram pattern recognition for control of powered upper-limb prostheses: State of the art and challenges for clinical use. Journal of Rehabilitation Research and Development, 48(6), 643–659. https://doi.org/10.1682/JRRD.2010.09.0177

3. Farina, D., Jiang, N., Rehbaum, H., Holobar, A., Graimann, B., Dietl, H., & Aszmann, O. C. (2014). The extraction of neural information from the surface EMG for the control of upper-limb prostheses: Emerging avenues and challenges. IEEE Transactions on Neural Systems and Rehabilitation Engineering, 22(4), 797–809. https://doi.org/10.1109/TNSRE.2014.2305111

4. Parajuli, N., Sreenivasan, N., Bifulco, P., Cesarelli, M., Savino, S., Niola, V., Esposito, D., Hamilton, T. J., Naik, G. R., Gunawardana, U., & Gargiulo, G. D. (2019). Real-time EMG-based pattern recognition control for hand prostheses: A review on existing methods, challenges, and future implementation. Sensors, 19(20), 4596. https://doi.org/10.3390/s19204596

5. Englehart, K., & Hudgins, B. (2003). A robust, real-time control scheme for multifunction myoelectric control. IEEE Transactions on Biomedical Engineering, 50(7), 848–854. https://doi.org/10.1109/TBME.2003.813539

6. Li, W., Shi, P., & Yu, H. (2021). Gesture recognition using surface electromyography and deep learning for prostheses hand: State-of-the-art, challenges, and future. Frontiers in Neuroscience, 15, 621885. https://doi.org/10.3389/fnins.2021.621885

7. Kyranou, I., Vijayakumar, S., & Erden, M. S. (2018). Causes of performance degradation in non-invasive electromyographic pattern recognition in upper limb prostheses. Frontiers in Neurorobotics, 12, 58. https://doi.org/10.3389/fnbot.2018.00058

8. Simon, A. M., Newkirk, K., Miller, L. A., Turner, K. L., Brenner, K., Stephens, M., & Hargrove, L. J. (2024). Implications of EMG channel count: Enhancing pattern recognition online prosthetic testing. Frontiers in Rehabilitation Sciences, 5, 1345364. https://doi.org/10.3389/fresc.2024.1345364

9. Aghchehli, E., Jabbari, M., Ma, C., Dyson, M., & Nazarpour, K. (2025). Medium density EMG armband for gesture recognition. Frontiers in Neurorobotics, 19, 1531815. https://doi.org/10.3389/fnbot.2025.1531815

10. Leone, F., Gentile, C., Ciancio, A. L., Gruppioni, E., Davalli, A., Sacchetti, R., Guglielmelli, E., & Zollo, L. (2019). Simultaneous sEMG classification of hand/wrist gestures and forces. Frontiers in Neurorobotics, 13, 42. https://doi.org/10.3389/fnbot.2019.00042

11. Leone, F., Mereu, F., Gentile, C., Cordella, F., Gruppioni, E., & Zollo, L. (2023). Hierarchical strategy for sEMG classification of the hand/wrist gestures and forces of transradial amputees. Frontiers in Neurorobotics, 17, 1092006. https://doi.org/10.3389/fnbot.2023.1092006

12. Stefanelli, E., Mohammadi, A., Wang, C., Yu, T., Tan, Y., Choong, P., Cordella, F., Zollo, L., & Oetomo, D. (2026). Simultaneous recognition of hand gestures, grasping force, and hand aperture using a wearable displacement myography system. IEEE Sensors Journal. Advance online publication. https://doi.org/10.1109/JSEN.2026.3679042

13. Zhou, C., Gao, Y., Gou, X., Yao, J., Wu, Q., Cao, D., He, X., & Yi, J. (2026). Feature-level fusion of surface electromyography and mechanomyography signals for MVC-normalized shoulder abduction force-level classification in healthy adults. Sensors, 26(14), 4351. https://doi.org/10.3390/s26144351

14. Billardello, R., Dejanovic, K., Cordella, F., D'Accolti, D., Cipriani, C., & Zollo, L. (2026). Hierarchical classification of EMG signal for hand and wrist gestures and forces in myoelectric control. IEEE Transactions on Neural Systems and Rehabilitation Engineering, 34, 978–987. https://doi.org/10.1109/TNSRE.2026.3660210

15. Atzori, M., Gijsberts, A., Castellini, C., Caputo, B., Mittaz Hager, A.-G., Elsig, S., Giatsidis, G., Bassetto, F., & Müller, H. (2014). Electromyography data for non-invasive naturally-controlled robotic hand prostheses. Scientific Data, 1, 140053. https://doi.org/10.1038/sdata.2014.53PubMed

16. Dai, Q., Wong, Y., Kankanhalli, M., Li, X., & Geng, W. (2023). Improved network and training scheme for cross-trial surface electromyography (sEMG)-based gesture recognition. Bioengineering, 10(9), 1101. https://doi.org/10.3390/bioengineering10091101

17. Qiu, F., Liu, X., & Ye, X. (2025). Influence of electrode placement on the recognition of different gesture categories using high-density sEMG. Frontiers in Neuroscience, 19, 1750792. https://doi.org/10.3389/fnins.2025.1750792

18. Smith, L. H., Hargrove, L. J., Lock, B. A., & Kuiken, T. A. (2011). Determining the optimal window length for pattern recognition-based myoelectric control: Balancing the competing effects of classification error and controller delay. IEEE Transactions on Neural Systems and Rehabilitation Engineering, 19(2), 186–192. https://doi.org/10.1109/TNSRE.2010.2100828

19. Niu, X., Zhang, D., Qu, C., Ren, L., Qian, Z., Wu, J., Wang, K., & Ren, L. (2026). Decoding hand gestures under arm movements based on electromyography and acceleration signals. Journal of Bionic Engineering, 23(2), 880–897. https://doi.org/10.1007/s42235-026-00858-1

20. Shinde, A., Shete, V., & Mehendale, N. (2026). Confidence-gated temporal voting for EMG-based prosthetic arm control: A low-cost end-to-end pipeline with quantified rejection behaviour. Frontiers in Rehabilitation Sciences, 7, 1864998. https://doi.org/10.3389/fresc.2026.1864998

21. Yamamoto, M., Chung, K. C., Sterbenz, J., Shauver, M. J., Tanaka, H., Nakamura, T., Oba, J., Chin, T., & Hirata, H. (2019). Cross-sectional international multicenter study on quality of life and reasons for abandonment of upper limb prostheses. Plastic and Reconstructive Surgery Global Open, 7(5), e2205. https://doi.org/10.1097/GOX.0000000000002205

22. Resnik, L., Borgia, M., & Clark, M. (2020). Function and quality of life of unilateral major upper limb amputees: Effect of prosthesis use and type. Archives of Physical Medicine and Rehabilitation, 101(8), 1396–1406. https://doi.org/10.1016/j.apmr.2020.04.003

23. Wang, H., Li, N., Gao, X., Jiang, N., & He, J. (2024). Analysis of electrode locations on limb condition effect for myoelectric pattern recognition. Journal of NeuroEngineering and Rehabilitation, 21, 177. https://doi.org/10.1186/s12984-024-01466-y

24. Rasines, I., Prada, M., Bobrov, V., Agrawal, D., Martinez, L., Iriondo, P., Remazeilles, A., & McIntyre, J. (2021). Regulating grip forces through EMG-controlled prostheses for transradial amputees. Applied Sciences, 11(23), 11199. https://doi.org/10.3390/app112311199

25. Jiang, N., Chen, C., He, J., Meng, J., Pan, L., Su, S., & Zhu, X. (2023). Bio-robotics research for non-invasive myoelectric neural interfaces for upper-limb prosthetic control: A 10-year perspective review. National Science Review, 10(5), nwad048. https://doi.org/10.1093/nsr/nwad048

Беткей электромиография сигналдары арқылы қолмен ұстау түрі мен субъективті түрде белгіленген күш салу деңгейін әр қатысушыға бейімдеп тану: Қолдың туа біткен немесе жүре пайда болған болмауы жағдайында протездеуде қолдануға бағытталған пилоттық зерттеу

Асылбекова А. [1], Жолтаев Д.М. [2], Ожикенова А. [3], Алимбаева Ж. [4], Байжунусов Э.А. [5], Шайхиев С.С. [6], Ожикен А. [7*]

[1] Студент (қолданбалы жасанды интеллект бойынша MSc), Жасанды интеллект және деректер ғылымы мектебі, Astana IT University, Астана, Қазақстан. E-mail: ayaulymassylbekova35@gmail.com

https://doi.org/10.52889/1684-9280-2026-77-5-jto067

[2] Ассистент-профессор, Жасанды интеллект және деректер ғылымы мектебі, Astana IT University, Relive Research, Астана, Қазақстан. E-mail: darkhan.zholtayev@astanait.edu.kz
[3] Директор, Qazaq Youth Science Hub, Алматы, Қазақстан. E-mail: a.ozhikenova@satbayev.university
[4] Жетекші ғылыми қызметкер, Сәтбаев университеті, Алматы, Қазақстан. E-mail: zh.alimbayeva@satbayev.university
[5] Басқарма төрағасы, Салидат Қайырбекова атындағы Денсаулық сақтауды дамыту ұлттық ғылыми орталығы, Астана, Қазақстан. E-mail: e.baizhunussov@nrchd.kz
[6] Басқарма төрағасының орынбасары, Салидат Қайырбекова атындағы Денсаулық сақтауды дамыту ұлттық ғылыми орталығы, Астана, Қазақстан. E-mail: s.shaikhiyev@nrchd.kz
[7] Оқытушы, Qazaq Youth Science Hub, Алматы, Қазақстан. E-mail: a.ozhiken@satbayev.university

Түйіндеме

Зерттеудің мақсаты: Қолды туа біткен немесе жүре пайда болған себептермен жоқ ересектерде беткей электромиография сигналдары арқылы ұстау түрі мен субъективті түрде белгіленген күш салу деңгейін әр қатысушыға бейімдеп тану мүмкіндігін бағалау және басқару ниетінсіз жасалған күнделікті қимылдар кезіндегі күтпеген шығыстарды анықтау. Зерттеу қолы туа біткен немесе жүре пайда болған себептерден жоқ адамдарға арналған протезді басқару технологиясын әзірлеудің бастапқы кезеңі болып табылады.

Әдістері. Жоғарғы аяқ-қолы ампутацияланбаған 4 ересек қатысушы 8 пәрмен күйін орындады: тыныштық, қолды ашу, сондай-ақ ауызша нұсқау бойынша төмен, орташа және жоғары күш салу деңгейімен толық алақанмен және саусақ ұштарымен ұстау. Күш салу деңгейлері субъективті болды, механикалық күш өлшенген жоқ. Әр қатысушы үшін сигналдың бірізді терезелерінен алынған уақыттық белгілер бойынша жеке сызықтық дискриминанттық талдау моделі оқытылды. Шығыстар 20 терезе бойынша каузалды көпшілік дауыс беру арқылы біріктірілді. Бағалау модельді оқытудан бөлінген сынақтарды, жаңадан жазылған пәрмендерді және басқару ниетінсіз жасалған күнделікті қимылдарды қамтыды. Соңғысына 0,60 сенімділік шегі ретроспективті қолданылды. Барлық жазбалар бір келу кезінде алынды, физикалық протез іске қосылған жоқ.

Нәтижесі. Кейінге қалдырылған сынақтарда орташа теңдестірілген дәлдік бастапқы терезелерде 0,810, көпшілік дауыс беруден кейін 0,823 және сынақ деңгейінде 0,875 болды. Ұстау түрі дұрыс танылған шығыстарда күш салу деңгейі толық алақанмен ұстау кезінде 0,970, ал саусақ ұштарымен ұстауда 0,706 дәлдікпен танылды. Жаңадан жазылған сынақтарда орташа теңдестірілген дәлдік 0,902, сынақ деңгейіндегі дәлдік 0,939 болса, ал сенімділік шегінде қамту 0,925 және жалпы дәлдік 0,862 болды. Күнделікті қимылдарда күтпеген белсенді шығыстардың орташа үлесі 35,6%-дан сенімділік бойынша қабылдамаудан кейін 22,3%-ға төмендеді, шығыстардың 81,3%-ы сақталды. Ең ұзақ үздіксіз белсенді шығыс 7,25 секундқа созылды.

Қорытынды. Бақыланатын жағдайда әр қатысушыға бейімделген модель берілген ұстау және күш салу пәрмендерін таныды. Күнделікті қимылдар кезіндегі күтпеген шығыстар протезде қолданудың ықтимал шектеуін көрсетеді. Нәтижелер клиникалық пайдасын немесе протезді басқаруды дәлелдемейді. Мақсатты пайдаланушылардың қатысуымен, физикалық протезбен және функционалдық тапсырмалармен қосымша бағалау қажет.

Түйін сөздер: электромиография, жасанды аяқ-қолдар, машиналық оқыту, тағылатын электрондық құрылғылар, дискриминанттық талдау, жоғарғы аяқ-қол.

Индивидуальное распознавание типа хвата и субъективно заданного уровня усилия по сигналам поверхностной электромиографии: Пилотное исследование для применения в протезировании при врожденном или приобретенном отсутствии верхней конечности

Асылбекова А. [1], Жолтаев Д.М. [2], Ожикенова А. [3], Алимбаева Ж. [4], Байжунусов Э.А. [5], Шайхиев С.С. [6], Ожикен А. [7*]

[1] Студент (MSc по прикладному искусственному интеллекту), Школа искусственного интеллекта и науки о данных, Astana IT University, Астана, Казахстан. E-mail: ayaulymassylbekova35@gmail.com
[2] Ассистент-профессор, Школа искусственного интеллекта и науки о данных, Astana IT University, Relive Research, Астана, Казахстан. E-mail: darkhan.zholtayev@astanait.edu.kz
[3] Директор, Qazaq Youth Science Hub, Алматы, Казахстан. E-mail: a.ozhikenova@satbayev.university
[4] Ведущий научный сотрудник, Сатпаев Университет, Алматы, Казахстан. E-mail: zh.alimbayeva@satbayev.university

https://doi.org/10.52889/1684-9280-2026-77-5-jto067

[5] Председатель Правления, Национальный научный центр развития здравоохранения имени Салидат Каирбековой, Астана, Казахстан. E-mail: e.baizhunussov@nrchd.kz
[6] Заместитель Председателя Правления, Национальный научный центр развития здравоохранения имени Салидат Каирбековой, Астана, Казахстан. E-mail: s.shaikhiyev@nrchd.kz
[7] Преподаватель, Qazaq Youth Science Hub, Алматы, Казахстан. E-mail: a.ozhiken@satbayev.university

Резюме

Цель исследования: оценить возможность индивидуального распознавания типа хвата и субъективно задаваемого уровня усилия по данным поверхностной электромиографии у взрослых без ампутации верхней конечности, а также выявить непреднамеренные выходы при обычных движениях. Исследование рассматривается как предварительный этап разработки управления протезом для людей с врожденным или приобретённым отсутствием верхней конечности.

Методы. Четыре взрослых участника без ампутации верхней конечности выполняли восемь командных состояний: покой, раскрытие кисти, а также силовой и щипковый хват при низком, среднем и высоком усилии по вербальной инструкции. Категории усилия были субъективными; механическая сила не измерялась. Для каждого участника обучали отдельную модель линейного дискриминантного анализа на временных признаках последовательных окон сигнала, после чего применяли каузальное мажоритарное голосование по двадцати окнам. Оценка включала отложенные испытания, отделенные от обучения, новые записанные командные испытания и обычные движения без намерения управлять. К последним ретроспективно применяли порог уверенности 0,60. Все записи получены за один визит; физический протез не приводился в действие. Результаты обобщали описательно.

Результаты. В отложенных испытаниях средняя сбалансированная точность составила 0,810 для исходных окон, 0,823 после мажоритарного голосования и 0,875 для решений на уровне испытаний. Среди выходов с правильно распознанным типом хвата усилие распознавалось точнее при силовом хвате (0,970), чем при щипковом (0,706). В новых испытаниях средняя сбалансированная точность составила 0,902, точность на уровне испытаний — 0,939; при пороге уверенности охват достиг 0,925, сквозная точность — 0,862. При обычных движениях средняя доля непреднамеренных активных выходов снизилась с 35,6% до 22,3% после отбраковки по уверенности, при которой сохранялось 81,3% всех выходов. Самый длинный непрерывный эпизод активного выхода после отбраковки длился 7,25 секунды.

Выводы. В контролируемых условиях индивидуальный декодер распознавал заданные команды хвата и усилия. Непреднамеренные выходы при обычных движениях остаются ограничением для потенциального применения в протезировании. Результаты не доказывают клиническую пользу или возможность управления протезом; необходимы исследования с участием целевых пользователей, физическими протезами и функциональными заданиями.

Ключевые слова: электромиография, искусственные конечности, машинное обучение, носимые электронные устройства, дискриминантный анализ, верхняя конечность.

https://doi.org/10.52889/1684-9280-2026-77-5-jto067